Supplementary Information

Nanoscale charge distribution and energy band modification in defect-patterned graphene

Shengnan Wang, [a,b]‡ **Rui Wang,** [a,c]‡ **Xiaowei Wang,** [a] **Dongdong Zhang,** [a,c] **and Xiaohui Qiu** [a]*

a National Center for Nanoscience and Technology, No.11 ZhongGuanCun BeiYiTiao, Beijing, China.

b Department of Physics, Tsinghua University, Haidian District, Beijing, China.

c Academy of Advanced Interdisciplinary Studies, Peking University, No.5 Yiheyuan Road Haidian District, Beijing, China

A. Estimation of tip-sample capacitance.

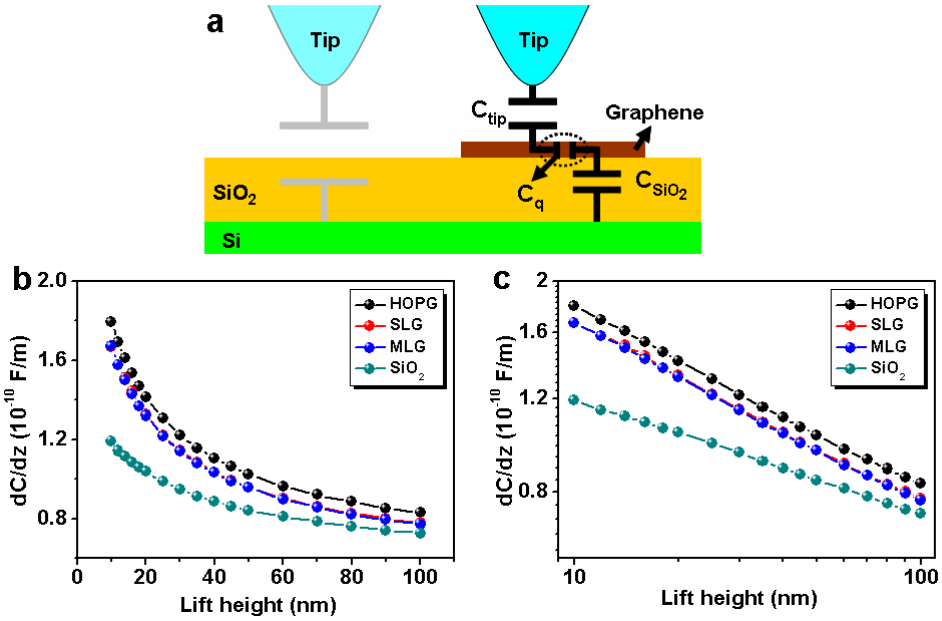

Figure S1. (a) Illustration of the capacitance model of tip on graphene sample. (b) dC/dz *vs* z plots on HOPG, SLG, BLG, and SiO_2, respectively. (c) Log-log plot of dC/dz *vs* z corresponded to (b). The observed linear feature indicates the power law dependence of dC/dz on z, which is dominant by the shape of probe usually taken as a "cantilever - cone- sphere" model .[1,2]

For the configuration of probe/air/graphene/SiO_2/n^+Si capacitor, the total capacitance C is the series of the tip geometric capacitance C_{tip}, the graphene quantum capacitance C_q, and the geometric capacitance of SiO_2 (C_{SiO_2}). The C_q is related to the density of state and the effective screening area

of graphene, usually much larger than C_{tip} and C_{SiO_2}, thus the contribution of C_q can be ignored in the series capacitor.[3] The absolute capacitance value can be obtained from the plot of dC/dz on the dependence of tip lift height.[1] The EFM tip has a capacitance of $\sim 9 \times 10^{-18}$ F when tip lifts up 10nm on the surface of highly ordered pyrolytic graphite (HOPG).

B. Analysis of structure and chemical contains in GO and rGO.

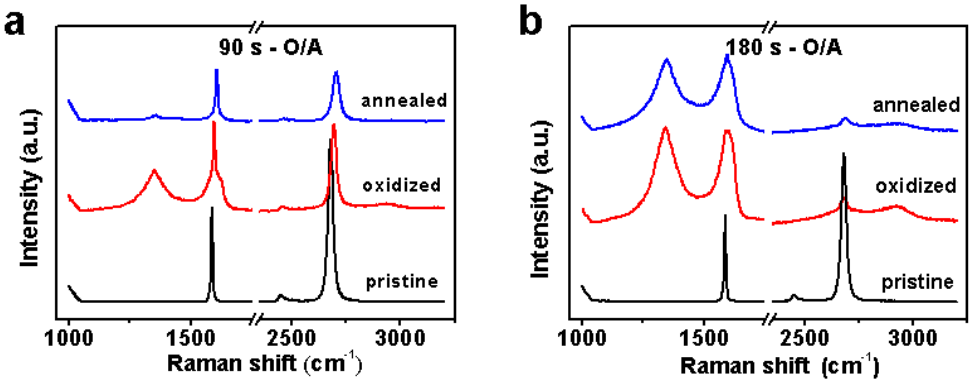

Figure S2. Raman spectra acquired on SLG samples subjected to different oxidation time: (a) 90s oxidation, (b) 180s oxidation; and followed by thermal annealing.

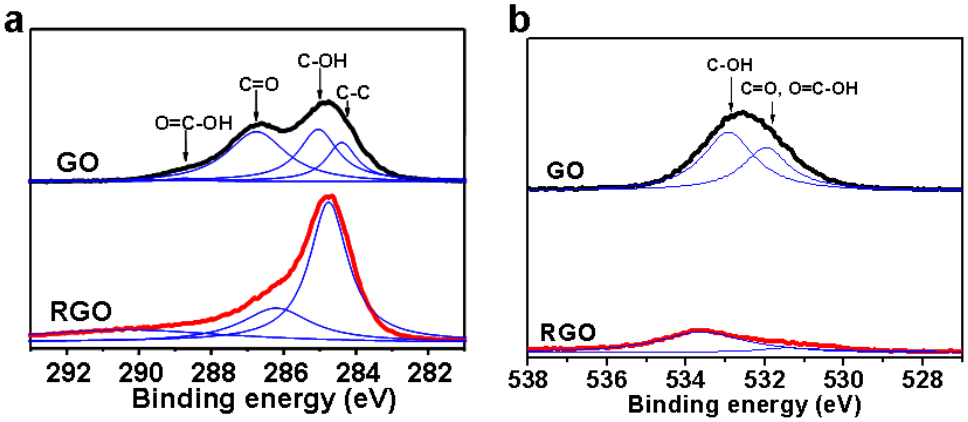

Figure S3. XPS spectra of GO sample (chemically derived from Hummers methods) before and after 500℃ annealing in vacuum. (a) Comparison of C1s peaks of GO and RGO. (b) Comparison of O1s peaks of GO and RGO.

The Raman spectra shows that the D and D' bands of SLG oxidized for 90s could be significantly reduced after the thermal annealing. In contrast, the defects present in SLG oxidized for

180s seem to be more energetically stable. The D and D' bands were still pronounced after the annealing process. Our XPS data showed a drastic decrease of oxygen-related bands of GO (derived from Hummers' methods) at high temperature, indicating that the oxygen atoms are significantly removed by thermal annealing. Recently, Larciprete et al introduced a dual path mechanism in the thermal reduction of GO that driven by the oxygen coverage.[4] For the moderately oxidized graphene, oxygen atoms adsorbed as epoxy groups and desorbed as O_2 leaving the carbon network undestroyed. For the extensively oxidized graphene, the oxygen atoms would react with the surrounding carbon atoms at high temperature, which consume the C backbone. The remained defect-bands of 180s oxidized graphene after annealing were indicative of the large amount of structural defects.

C. Discussion of band gap in GO and rGO.

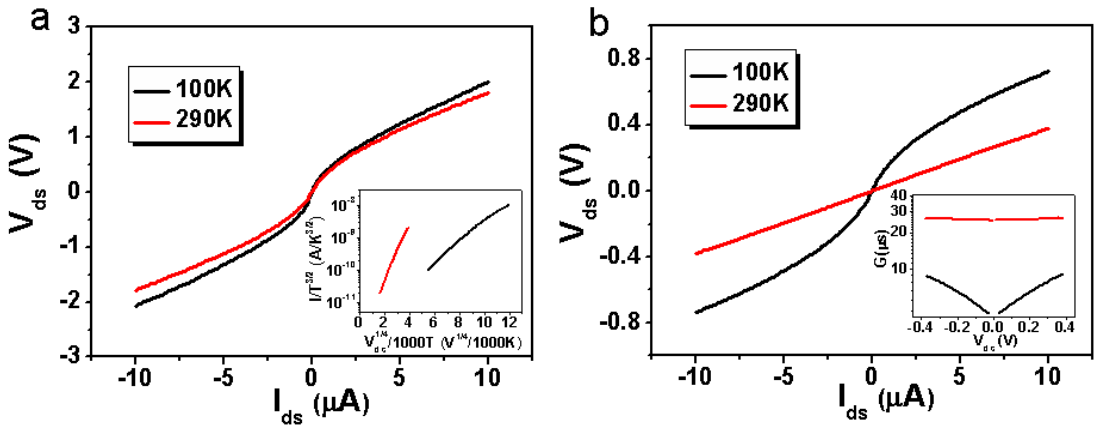

Figure S4. Nonlinear transport characteristics of (a) G/GO/G and (b) G/rGO/G junctions at 100K and 300K corresponded to the same device in Figure 5. The inset of (a) presents $I/T^{3/2}$ as a function of $V_{ds}^{1/4}/T$. The observed linear dependence in this plot is interpreted as an inversely biased Schottky diode behavior that the current is determined by the themionic emission. The inset of (b) is logarithmic scale of conductance $G=I_{ds}/V_{ds}$ as a function of V_{ds}, the linear dependence of log (G) vs V_{ds} is respected to the 2D VRH transport behavior.

The G/GO/G junctions are commonly considered as two back to back Schottky barriers. The current through these junctions is dominated by the thermionic emission over the negative biased

Schottky birrier, which can be fitted by $I_{ds} \propto T^{3/2}\exp((\alpha V_{ds}^{1/4}-\phi_b)/T)$, where $\alpha=q/k_B \times[(q^3N_d)/(8\pi(\varepsilon')^2\varepsilon)]^{1/4}$ is a constant related to the dielectric constant and the Boltzmann's constant. N_d is the ionized donor density, ϕ_b is the effective Schottky barrier height formed at the interface of GO and metal, T is the temperature. I-V curves are dependent on the T, and the ϕ_b is fitted to be 0.6eV and 0.2eV at 290K and 100K, respectively. The conductance in rGO is dominated by the electron hopping between the conductive graphene islands separated by the insulating barriers. The conductance is dependence on the hopping distance and the bias electric field as described by $G \propto \exp(-\frac{r(T)}{k_B T})$, where r(T) is the mean low-field hopping distance that represented as the slope of the curves in the inset of Figure S4b. r(T) is strongly dependent on the temperature. In this G/rGO/G junctions, the r(T) is nearly zero at 290K according to the linear transport characteristics, which means the energy barrier is below than ~30meV for electron hopping.

References

S1. Cherniavskaya, O.; Chen, L. W; Weng, V.; Yuditsky, L.; Brus, L. E. Quantitative noncontact electrostatic force imaging of nanocrystal polarizability. *Journal of Physical Chemistry B* **2003**, 107, 1525.

S2. Colchero, J.; Gil, A; Baró, A. M.; Resolustion enhancement and improved data interpretation in electrostatic force microscopy. *Phys. Rev. B* **2001**, 64, 245403.

S3. Fang, T.; Konar, A.; Xing, H.; Jena, D. Carrier statistics and quantum capacitance of graphene sheets and ribbons. *Appl. Phys. Lett.* **2007**, 91, 092109.

S4. Larciprete, R.; Fabris, S.; Sun, T.; Lacovig, P.; Baraldi, A.; Lizzit, S. Dual path mechanism in the thermal reduction of graphene oxide. *J. Am. Chem. Soc.* **2011**, DOI: 10.1021/ja205168x.